

## On-Line Prediction of Dry Zones During Composite Process Through Digital Shadow Approach

LE BOT Philippe<sup>1,a\*</sup>, LAUZERAL Nathan<sup>1,b</sup>, FOUICHE Olivier<sup>1,c</sup>,  
SIDDIG Nihad<sup>1,d</sup>, LECOINTE Damien<sup>1,e</sup>, ABDULLAH Ibrahim<sup>1,f</sup>,  
NIGET Florent<sup>1,g</sup> and MARCHAND Christophe<sup>1,h</sup>

<sup>1</sup>Nantes Université, IRT Jules Verne, 1 mail des 20000 lieues, 44340 BOUGUENNAIS

<sup>a</sup>Philippe.le-bot@irt-jules-verne.fr (\*corresponding author), <sup>b</sup>nathan.lauzeral@irt-jules-verne.fr,  
<sup>c</sup>olivier.fouche@irt-jules-verne.fr, <sup>d</sup>nihad.siddig@irt-jules-verne.fr,  
<sup>e</sup>damien.lecointe@irt-jules-verne.fr, <sup>f</sup>ibrahim.abdullah@irt-jules-verne.fr,  
<sup>g</sup>florent.niget@irt-jules-verne.fr, <sup>h</sup>christophe.marchand@irt-jules-verne.fr

**Keywords** Process monitoring, digital shadow, composites.

**Abstract.** A novel solution for monitoring the infusion process and providing decision support to operators involved in the manufacturing of large, unique or near-unique parts is presented. Based on a scientific approach referred to as the 5D methodology (D for dimensions), the proposed solution consists of a process digital shadow built upon a metamodel that is fed in real time by signals from sensors embedded in the process, enabling the anticipation of defects such as dry spots.

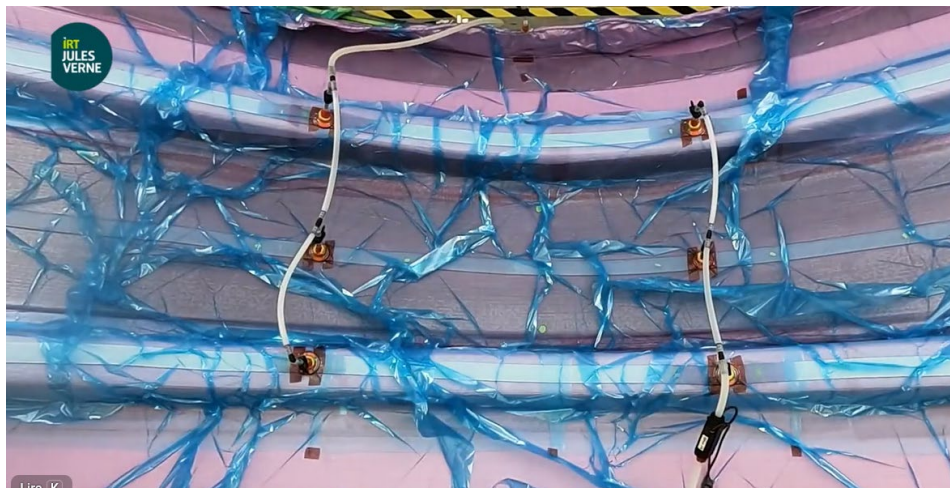


**Fig. 1.** Infusion of part – IRT Jules Verne – Project MONOCLE

### Introduction

Composite parts are becoming increasingly important in modern industrial structures. Forming processes, such as infusion, must enable the manufacture of parts with ever-higher mechanical performance. At the same time, the parts manufactured are both large and increasingly complex in shape and architecture. However, the appearance of defects such as “dry areas” (areas where the resin has not been able to impregnate the fiber reinforcement) significantly reduces the final properties of the part, which is unacceptable in many industrial fields. However, these dry areas are sometimes unpredictable (they appear randomly) or invisible to the operator. Monitoring the infusion process therefore appears to be an essential solution. There are many solutions available, based on sensors and industrial solutions[1-4] or more academic ones [5-7], but these solutions are descriptive, rarely predictive, and even less prescriptive and often based on large productions.

Our study deals with the infusion of (quasi) unique composite parts, with the aim of getting it right first time. Digital shadow tools, powered by a process metamodel, appear to be a particularly suitable solution. The metamodel integrated into the digital twin is used to describe the state of the system (machine, tooling, preform, resin) at time  $t$ , to predict the state of the same system at future times

$t+\Delta t$ , and finally to prescribe process adjustment modifications to improve the state of the system at that same future time  $t+\Delta t$ .

The following sections describe the various stages involved in constructing this digital shadow to limit dry areas: the overall method (known as the 5D approach), followed by each of its dimensions: Physical entities, virtual models, Digital shadow data, Services and Connections. Finally, the initial results are discussed.

## Procedure

Data management in the context of digital twins is a major challenge due to the lack of formalization, models, or conceptualization of the data lifecycle, despite growing interest from manufacturers. To address this challenge, A data lifecycle model and a data typology from academic literature [8] coupled with normative literature [10] have been used in this study to comprehensively characterize the different stages of data management. The resulting formalization of data management ensures the quality, consistency, and reliability of the data used in the various digital twin applications. It also makes it possible to scale the digital twin architecture in terms of resources (storage, computing power, transmission frequencies, etc.).

$$M_{DT} = (PE, VE, S_s, DD, CN)$$

where PE is a physical entity that exists in the real world. This includes tools, materials, sensors, and data acquisition tools. VE is the virtual dimension and contains all knowledge elements and models, including digital process simulation tools. Ss is a service provided by both PE and VE, DD is data that make up the digital twin and CN are the links between the different parts of the digital twin [9].

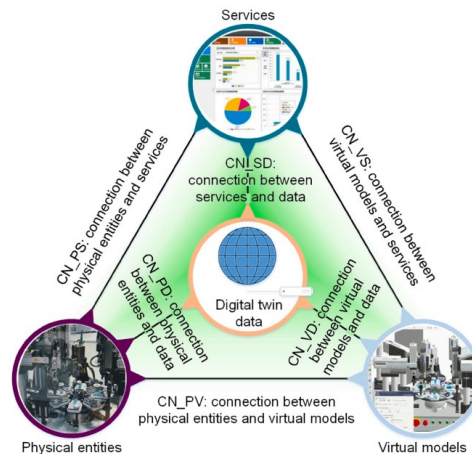


**Fig. 2.** Five-dimension digital twin mode [8]

This approach to the management of information flows between process-generated data and data derived from knowledge modeling enables the real-time updating of a metamodel through high-performance communication protocols. The service-oriented paradigm facilitates a focus on industrial objectives and is computationally formalized through the client–server architecture. In the following paragraphs, each of the five dimensions of the problem is explained in detail in order to arrive at a solution for a digital shadow of the infusion process.

### Dimension#1: Physical entities

#### 1. Labscale testbench

An infusion test bench (Figure 3) has been specially designed to analyze infusions on a laboratory scale. This bench can be used to evaluate sensors and infusion configurations, on plates or tools, as well as to test digital shadow solutions on a small scale. The expected functions of the test bench were determined by a functional analysis carried out by the consortium.

The infusion test bench is a mechanically welded and assembled piece of equipment used to study the composite infusion process for different part sizes and geometries. It consists of two assemblies:

- A main section that is mobile on four wheels and held in place by four foot-operated jacks.
- A mobile table on four wheels, held in place on the main equipment by two clamps.

A gantry moves along three axes, each controlled by an IGUS DRYVE D1 control card. A fixture is located at the end of the z-axis. The gantry is height-adjustable by means of a device with four LINAK electric cylinders controlled by a maintained action on the control devices provided for this purpose.

Several configurations are possible and were used during the project (Figure 4):

- Configuration 1: draping the part directly on the transparent marble slab.
- Configuration 2: tools directly on the transparent marble slab.
- Configuration 3: tools inside the marble.
- Configuration 4: tools near the marble.

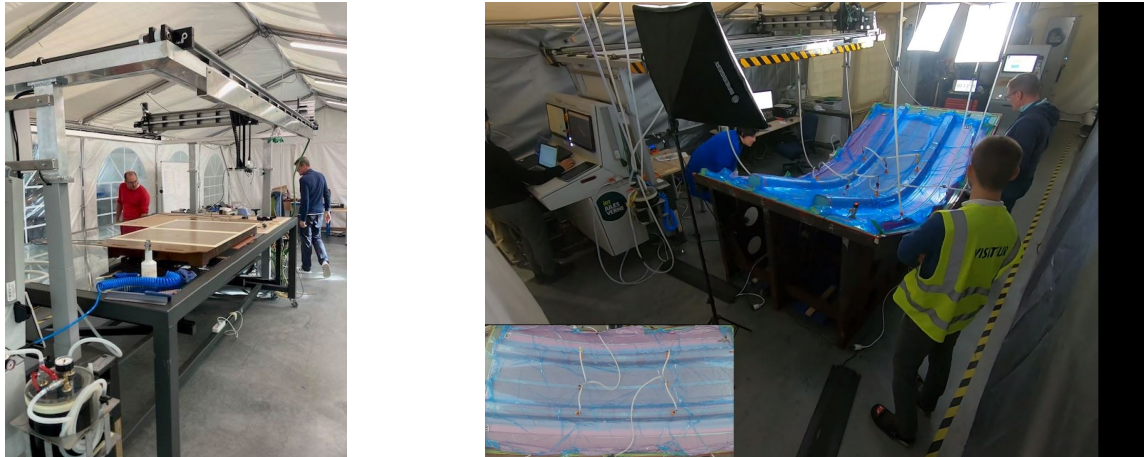


**Fig. 3.** Overview of the test bench in its environment in two different applications (tools on the marble surface on the left and tools on the side on the right)

## 2. Process sensors

The proposed solution for achieving right-first-time production of large composite parts relies on the deployment of multiple sensors to accurately characterize the process signature, which is captured and interpreted by a metamodel operating concurrently with the manufacturing process. Sensors are used either as inputs (e.g., model boundary conditions), outputs (verification of model relevance), or as process business indicators. There are many sensors available to perform these functions for the infusion process. In this study, a sensor selection procedure based on experimental campaigns conducted on the lab-scale test bench was implemented. The sensors ultimately selected, based on criteria related to the sensitivity of the signals obtained, the possibility of performing automated analyses, and compatibility with the data acquisition system, are as follows: a camera (in the visible spectrum), a resin flowmeter, a vacuum sensor, and a heat flux and temperature sensor placed on the vacuum bag. Other sensors were tested but had major drawbacks in terms of one of the selection criteria.

- **Sensor #1: Camera (a2A5328-4gmBAS, BASLER)**

Its characteristics and mode of installation allow images to be acquired across an entire 6m<sup>2</sup> room with resolution of 1,5mm/pixel. The various tests carried out throughout the project demonstrated the importance of lighting in obtaining high-quality images that enable automatic segmentation of the resin front. Firstly, the images acquired must be uniform, with no areas that are overexposed or underexposed. Finally, the brightness must not vary during acquisition; tests must be carried out under controlled lighting conditions, away from sunlight. Specific work on lighting was therefore carried out. A concrete result from a plate infusion test is shown on the Figure 4.



**Fig. 4.** Infusion test of a plate with camera and lighting - experimental setup (left) and result of the infusion in progress (right)

Significant effort was devoted to intrinsic and extrinsic calibration procedures aimed at correcting image distortions and mapping the resulting data onto CAD models of the part being infused. This work was first validated on a flat plate and subsequently on a 6 m<sup>2</sup> simple-curved component (as proof of concept), under both laboratory and industrial lighting conditions.

The metamodels developed in this work do not directly exploit image data but rather resin front position data as a function of time. Consequently, an image segmentation algorithm was developed and deployed. The exploitation of the image flow obtained requires the use of deep learning to perform robust and adaptive segmentation of the resin front, without excessive dependence on experimental conditions (presence of shadows or unexpected objects). The DeepLabV3 model [11] was chosen for its ability to perform semantic segmentation. Given the limited data available to serve as a dataset for the model, we had to enrich this base with a set of synthetic data obtained artificially. The result is a highly effective segmentation algorithm that is robust under industrial conditions that are sometimes difficult to control. Subsequently, a real-time projection algorithm for the resin front obtained on a mesh of the part was developed. Figure 5 shows a concrete example of typical result of using a real-time camera during infusion on a 6m<sup>2</sup> test piece with a single curvature.

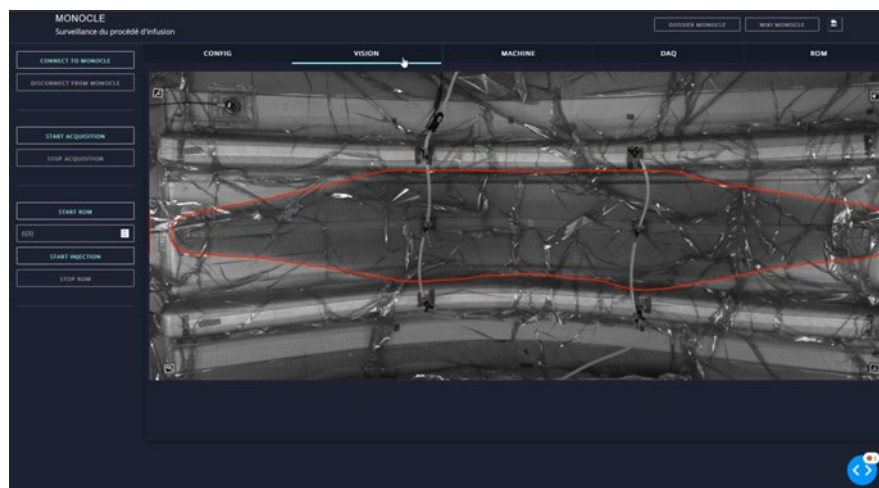


**Fig. 5.** Segmented resin front during infusion of the 6m<sup>2</sup> part (proof of concept)

- **Sensor #2: SDX20 flowmeter (Keyence)**

This sensor, mounted externally on the main resin supply hose, measures the volumetric flow rate of resin delivered to the preform. This measurement is used both as a validation criterion for numerical simulations and as an input for improving the metamodel and the resulting digital shadow. The two peaks in Figure 6 correspond to the openings of two ramps used during a plate infusion test, while an unexpected return to 0 at 700s corresponds to a signal loss due to too low a flow rate. A correction was systematically applied to remedy this problem and was used in all our tests.

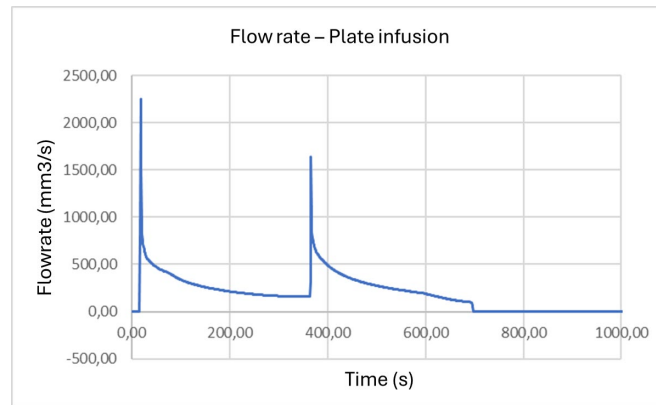


**Fig. 6.** Flowrate measurement during infusion process

- **Sensor #3: Vacuum pressure sensor**

These sensors measure pressure (or vacuum) via a ceramic membrane. Based on an initial commercial solution, the vacuum sensor has been modified so that the sensor membrane never comes into contact with environmental products or fiber reinforcement. A typical result is shown in Figure 7.

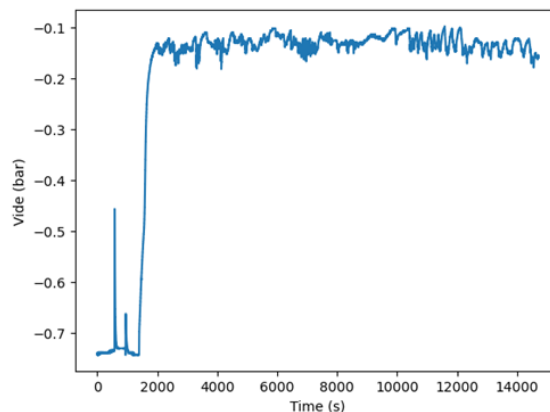


**Fig. 7.** Typical measurement of vacuum sensor during infusion process.

- **Sensor #4: Heat flux and temperature sensor – Tfx©**

The company Tfx has long developed a specific range of enthalpy heat flow sensors for Resin Transfer Molding and has more recently adapted this range of sensors for infusion [5]. Resin front detection is possible thanks to the change in thermal conductivity that occurs when the reinforcement is wetted. The infusion stage itself is often isothermal, so it is necessary to introduce a slight thermal gradient (1 to 2°C) across the composite to make the system sensitive to the wetting itself. It should be noted that this sensor does not measure “true” values but rather a quantity of the same unit and sensitivity. Nevertheless, the observable raw value is not the absolute value of the heat flow through the sensor but is a faithful representation of it. Figure 8 shows the results of a plate infusion test, for which two heat flux sensors are placed close to and far from the infusion point, respectively. The plates are made from a stack of plies with a total thickness of 10 mm. The resin is infused at 28°C, while the ambient temperature is 23°C. The infusion profile is classic, and the sensor near the infusion point detects the resin passing less than two minutes after the start of infusion. During the impregnation phase, there is a pronounced downward phase ( $-3000\text{W/m}^2$ ) if the sensor is located near the infusion point, and only  $-500\text{W/m}^2$  if it is located far away, followed by a return to zero. Just before passing in front of the sensor, the resin heats it up (increasingly negative flows) until it reaches thermal equilibrium with the resin/preform system (flow returns to zero). The resin then begins to polymerize, and the flow returns to negative values.

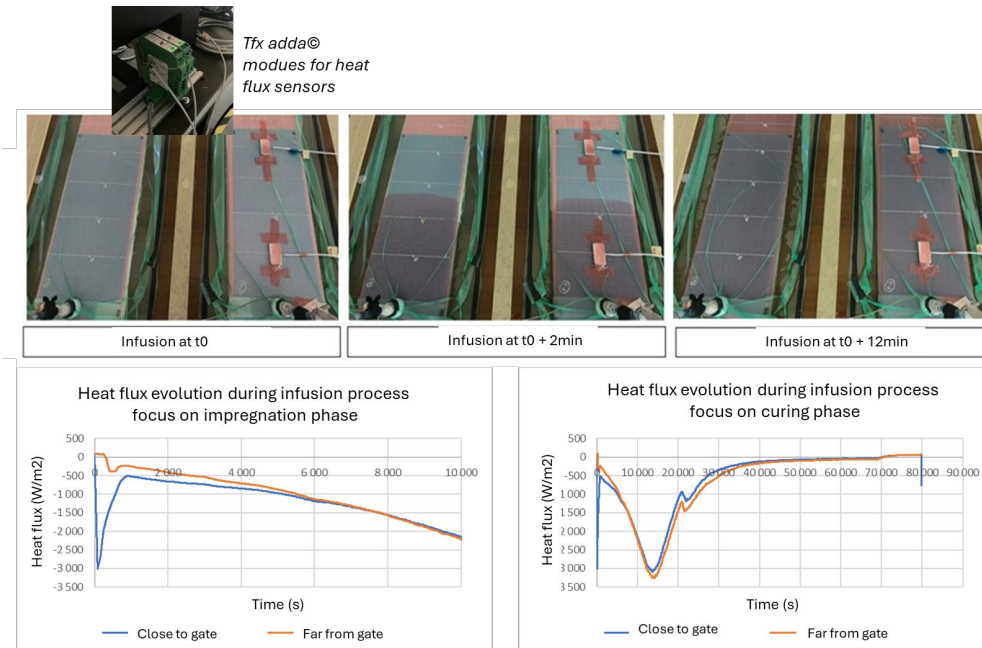


**Fig. 8.** Heat flux profile during plate infusion – Focus on the impregnation phase (left) and curing phase (right)

This example demonstrates the value and reliability of these sensors. They not only detect a resin front, but also quantify the progress of polymerization, despite the influence of their position relative to the injection points. They will serve both as performance metrics for the metamodel and as indicators for monitoring the progression of the reaction.

### Dimension #2: Virtual models

Since the goal is to have the first part good, there is, by definition, no experimental dataset that can be used to build a metamodel. Consequently, only a synthetic dataset derived from a set of reliable numerical simulations can replace a set of experimental tests. To perform these numerical simulations, several steps were necessary:

#### 1. Reinforcement properties measurements for high-fidelity process simulation

Two complementary approaches were either tested or developed:

- **Approach 1:** a digital methodology for permeability characterization is applied to a biaxial preform. First, the three-dimensional image of the material obtained by micro-computed tomography (micro-CT) was segmented. The complete three-dimensional permeability tensor was then computed using the PoroS software suite, developed by the laboratory GeM at Ecole Centrale de Nantes [14], based on a dual-scale flow simulation employing a Stokes–Brinkman solver.
- **Approach 2:** An experimental approach based on the simultaneous infusion of two plates in two different principal directions, with a set of relevant sensors (including strategically placed cameras), enabled the partial identification of the permeability tensor of the reinforcement under study to be identified using Darcy's equation.

A cross-validation step was successfully completed, enabling these preforms to be characterized with the expected accuracy (Figure 9).

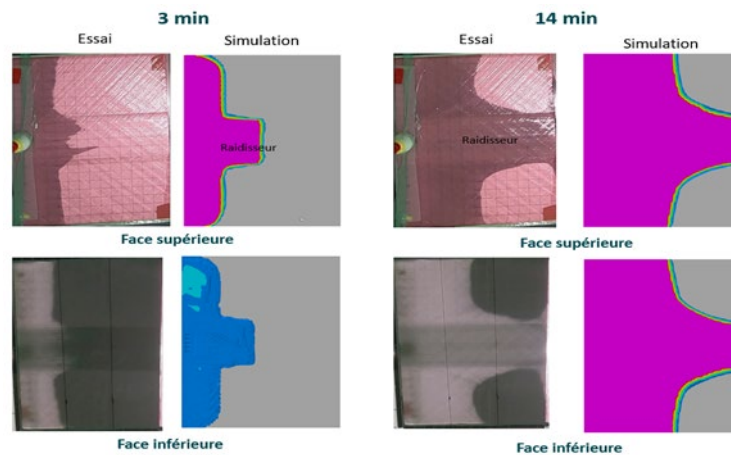


**Fig.9.** Comparison of tests/simulations for infusions using permeability tensor measured using the Jules Verne IRT protocol

## 2. Resin properties for high-fidelity process simulation

To model the behavior of the resin, a temperature-dependent viscosity law was integrated into the PAM-RTM© software, considering the ambient temperature and the initial temperatures of resin and reinforcement. Viscosity model, polymerization model and thermal properties—conductivity, heat capacity, and heat of reaction—were entered to enable calculation of the temperature and degree of polymerization during the cycle. These parameters ensure realistic simulation, considering the couplings between flow, heat transfer, and polymerization kinetics in both the filling phase and the polymerization phase.

## 3. Validation of high-fidelity process simulation accuracy with infusion experiments

All the models and material parameters are implemented in the process simulation tool PAM-RTM©. The experimental validation of simulations followed several steps depending on the part physical or geometrical complexities and the infusion strategy. Plates with a mono-thickness are addressed in previous publications [9].

### • Infusion of plates

Numerous cases (reference cases and cases with process variables such as the opening time of the second infusion ramp) were correlated with experiments conducted on the lab-scale test bench. The flow dynamics predicted by the simulation were systematically compared with the experiment during the filling phase (Figure 10), with good results in terms of accuracy and robustness in each case, but also with acceptable discrepancies explained by modeling imperfections and process variabilities.

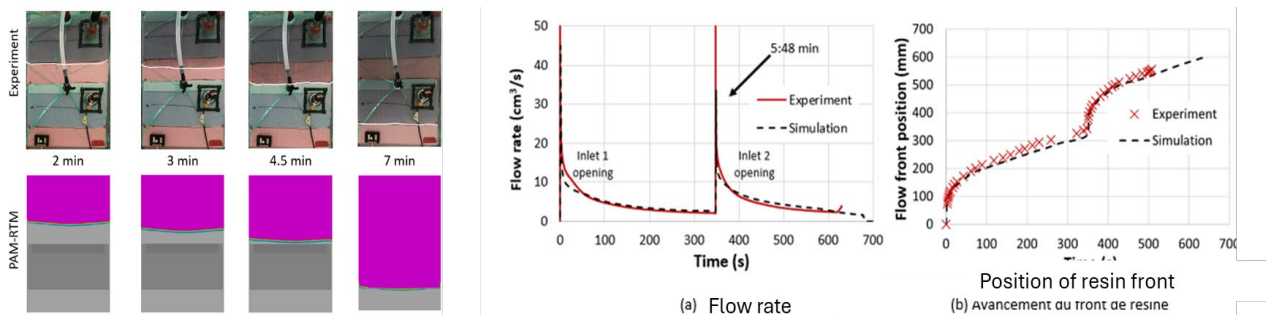


**Fig. 10.** Comparison between experimental and numerical advancement of the flow front

A specific test involving the infusion of a plate using two infusion ramps deals with opening the second infusion ramp at the same time as the first ramp in order to generate a dry zone. Figure 11 shows the experimental infusion test and the dry zones detected at the end of the process. This (non-

industrial) strategy resulted in two triangular dry areas in the first half of the part. A numerical simulation using the material parameters identified above and a strategy identical to the experiment shows dry areas of different sizes but identical positions. The accuracy obtained by the calculation is considered in this work to be sufficient for use in the development of a parametric metamodel.

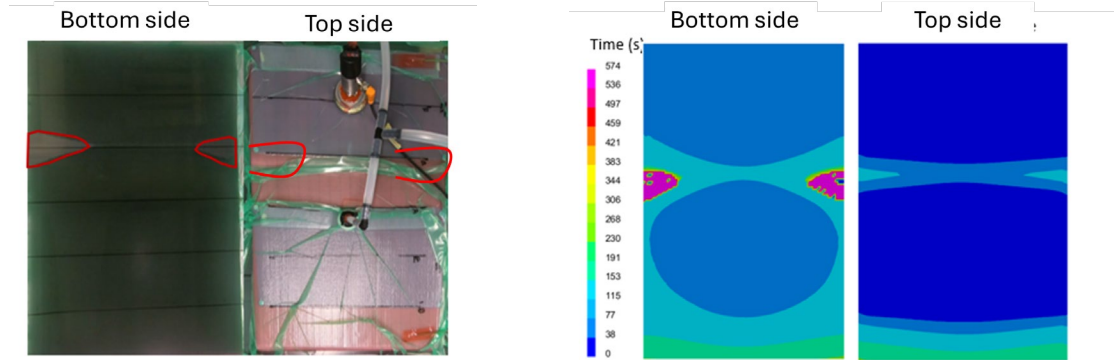


**Fig. 11.** Process simulation: Correlation between simulation and experiment on plate infusion with inclusion of voluntary dry spots.

- **Infusion of 6m<sup>2</sup> proof-of-concept part**

The proof-of-concept is a piece measuring approximately 6m<sup>2</sup> infused with two infusion points (ramp 1 in Figure 12) and equipped with two “emergency” ramps. The shape of the resin front predicted in the early stages of the experiment shows the accuracy of the simulation. It is this same shape that is identified for the digital shadow. This technical achievement in correlated digital simulation not only validated the expertise acquired in the digital simulation of the infusion process but is also useful as an essential starting point for the production of the synthetic data set required to develop the metamodel for the final digital shadow.

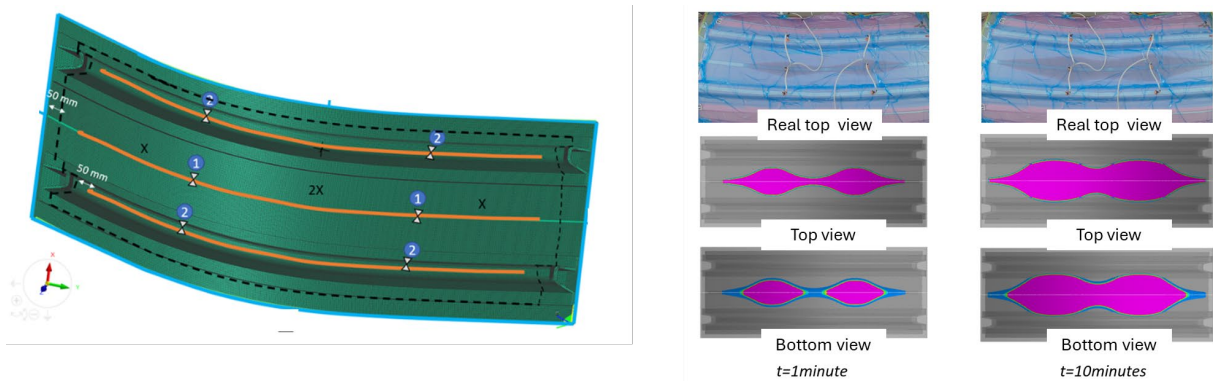


**Fig.12.** Comparison of simulation and experiment on a 6m<sup>2</sup> complex part with single curvature: mesh (left) and results over 1 min and 10 min (right)

### Dimension #3: Digital shadow data

#### 1. Development of the Computational Core

The computational core, hereafter referred to as the *metamodel*, is based on a deep learning approach and is implemented using the Python library PyTorch. The metamodel is developed with two main objectives:

- To enable real-time calibration using sensor data. In the present work, only the data provided by a camera observing the upper surface of the part are considered.
- To predict the flow-front dynamics, thereby allowing anticipation of the formation of dry spots.

- **Generation of training Data**

The metamodel is trained on a database of synthetic data generated using the PAM-RTM© software, presented in the previous Section.

The considered use case is as follows: a first set of infusion points is opened to initiate the filling of the part. At a given time  $\tau$ , a second set of infusion points is opened. The objective is to be able to predict the effect of this second opening on the formation of dry areas.

The design-of-experiments parameters were selected to accurately represent the flow-front propagation during infusion. Since a single simulation requires several hours of computation, the number of parameters was limited to two to achieve a robust sampling of the parametric space.

The selected parameters are:

- The opening time of the second set of injection valves,  $\tau$ . This parameter is mandatory since the ultimate goal is to optimize this opening time.
- The permeability in the direction perpendicular to the main flow,  $k_y$ . This parameter was identified as having a strong impact on the formation of dry spots. Furthermore, it allows an accurate representation of the flow-front shape visible to the camera. Since the model is calibrated solely from these observations, minimizing the representation error is critical.

Each simulation returns a field defined over 3D space  $(x, y, z)$  and time  $t$ . A single data sample therefore corresponds to the mapping  $(x, y, z, t, \tau, k_y) \rightarrow r$ , where  $r$  denotes the filling state. The flow front is represented as a binary field: true if resin is present, false otherwise. Both input and output data are normalized before being provided to the neural network. A total of 100 simulations were performed, with design-of-experiments parameters sampled using a Sobol sequence. Among them, 80 simulations are used for training and 20 for validation.

- **Architecture and Training**

The metamodel is developed using the concept of neural fields [12]. The selected architecture is a Multi-Layer Perceptron coupled with an initial positional encoding layer [13] enabling the capture of high-frequency behaviors.

The Adam optimizer and a binary cross-entropy loss are used to train the model. To assess the quality of the predictions, the Dice coefficient is employed, as the ground truth is binary. Moreover, since the primary objective is the accurate prediction of dry-spot formation, additional metrics such as the true positive rate and the number of false positives per image are also considered to assess the dry area detection.

- **Online Calibration**

Material parameters may be estimated prior to the experiment; however, the metamodel enables their real-time adjustment during the process. Although multiple sensor measurements are available, the metamodel interacts exclusively with the image provided by the camera, and more specifically with the segmented resin flow front on the upper surface of the part.

It is worth noting that, according to Darcy's law, viscosity can be interpreted as a weighting factor applied to the resin velocity throughout the part, since only a single resin type is used. As viscosity may be temperature-dependent, its correction is important. To this end, viscosity is replaced by a time-scaling parameter, denoted  $c_\mu$ , which effectively accelerates or decelerates the flow. Consequently, this parameter does not need to be included in the design of experiments.

At a given time  $t$ , the goal is therefore to estimate  $k_y$  and  $c_\mu$  based on the segmented flow front observed on the upper surface. The following inverse problem is solved:

$$(\widehat{k}_y, \widehat{c}_\mu) = \min_{k_y, c_\mu} \mathcal{L}^{inv} \left( f_\theta(x, y, z, t_0, k_y, c_\mu), \mathcal{S}(x, y, z, t_0) \right), \quad \forall (x, y, z) \in \Omega_d^v$$

where:

- the notation  $\hat{\cdot}$  denotes an estimated parameter,
- $f_\theta$  represents the metamodel,
- $\mathcal{S}(x, y, z, t_0)$  is the measured resin presence obtained from image segmentation,

- $\mathcal{L}^{inv}$  is the inverse-problem loss function, chosen here as the Dice coefficient,
- $t_0$  is the current time,
- $\Omega_d^v$  denotes the discretized spatial domain corresponding to the surface of the part visible by the camera.

Once the material parameters have been identified at time  $t_0$ , the metamodel can be evaluated at future times  $t > t_0$ . By varying the opening time  $\tau$  of the second injection manifold, it becomes possible to anticipate the formation of dry spots and support decision-making during the infusion process. An example of registration is shown Figure 13.

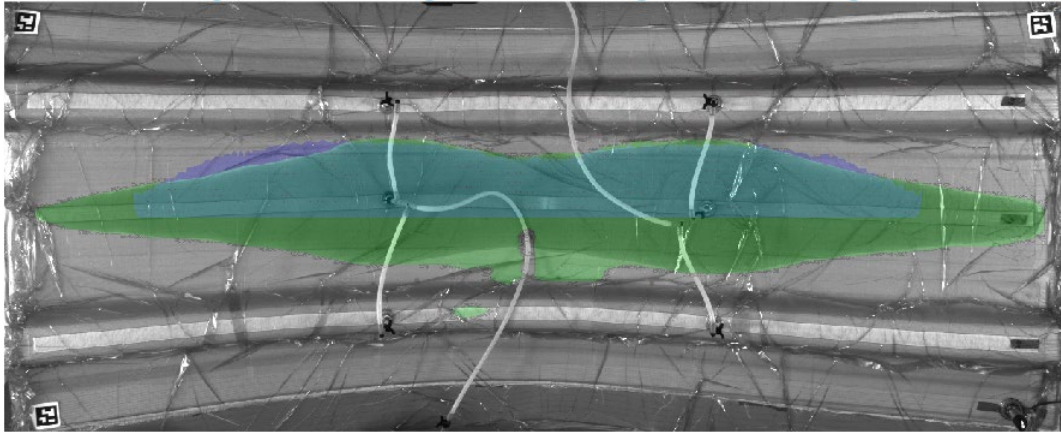


**Fig.13.** Resin flow-front segmentation and metamodel registration (with the camera image in black and white, the segmented resin region shown in green, the prediction associated with the mesh-to-pixel correspondence in dark blue, and their intersection in blue/green). Note, the metamodel prediction is volumetric and not limited to the surface.

#### Dimension#4: Connection

A data acquisition system (Figure 14) was specifically designed for this study so that it could integrate and synchronize the relevant sensors but also embed the metamodel and distribute information to the retrieval software. This system consists of

- A sensor data acquisition unit: This unit manages the acquisition of analog sensors in voltage (+/- 10V) and current (4-20 mA) as well as type K thermocouples.
- An industrial PC for processing, network management, and storage: The main functions integrated into this unit are
  - Management of data processing programs to manage:
    - Resin front monitoring by image analysis (vision module)
    - The AI model for predicting the infusion filling phase (prediction module)
  - Management of an OPCUA communication network to operate the connection with the infusion machine
- the connection between the various integrated modules (vision module and prediction module)
- the storage of infusion data

The two units are linked to each other by the OPCUA exchange protocol based on server/client approach.



**Fig. 14.** IRT Jules Verne data acquisition system

## Dimension#5: services

The aim of this work is to predict the appearance of dry spots during the process and to enable operators to take appropriate action in order to ultimately prevent them. The concept of service, implemented through a client–server approach to information flow, allows this objective to be addressed in a targeted manner. Commercial software (KASEM©), developed by IQANTO, Figure 15, was used for this purpose. It enables real-time visualization of process parameters and measurements, as well as real-time access to metamodel results. In addition, the metamodel can be configured to predict the appearance or disappearance of dry spots in response to changes in the infusion strategy, within a sufficiently short time frame (approximately ten seconds) to support operator decision-making.

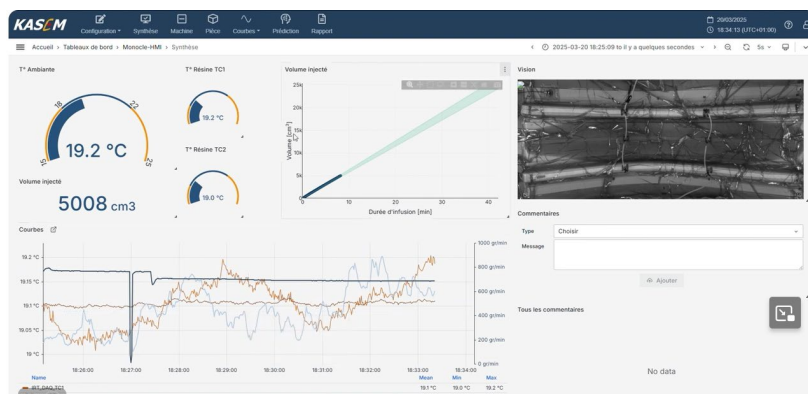


Fig. 15. Classical extract of specific Infusion GUI from KASEM©

In practical terms, for all validation examples presented hereafter, the infusion strategy provided as input to the metamodel is defined by the opening times of the infusion ramps, which can be advanced or delayed to avoid the formation of dry spots.

## Results and Discussion

### 1. Validation on plate

An initial validation test involves infusing a plate (200x400x10mm). The experimental setup is as follows (Figure 16): The part is first infused on one side, then via a ramp placed in the part's axis of symmetry. The following sensors were installed: a camera on the sheet side, a volume flow sensor, a Thermoflux© heat flux sensor, and a vacuum sensor. The parameters of the chosen numerical test plan are the opening time of the second valve  $\tau$ , and the permeability in the direction of flow of the drain. Experimentally, the second ramp is opened 150 seconds after the start of infusion.

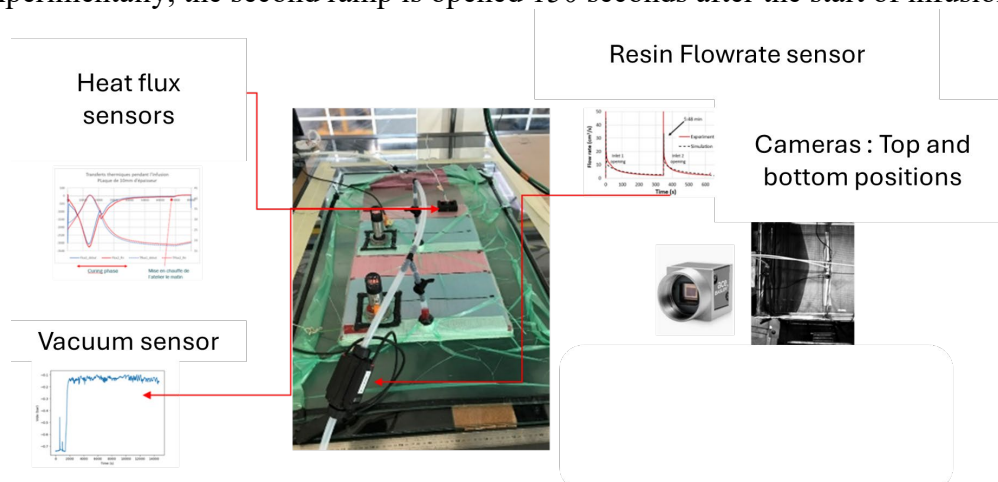
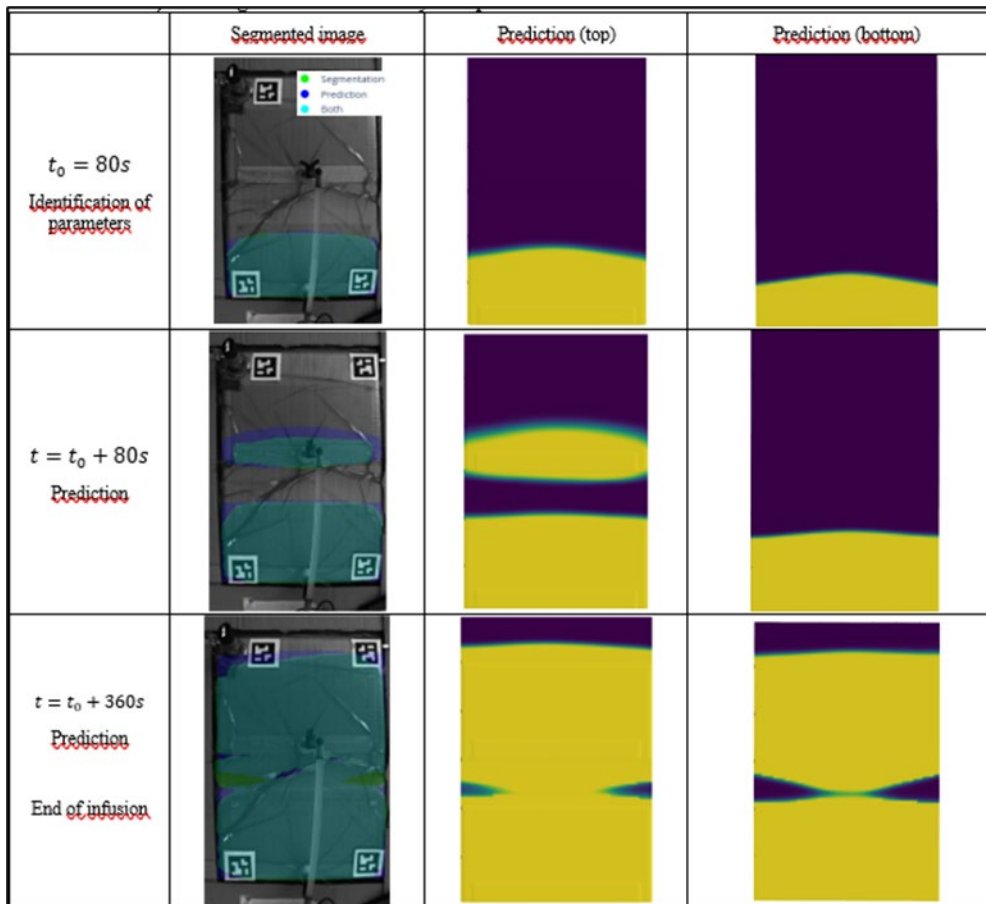


Fig. 16. Experimental validation on infused plate

Figure 17 provides an overview of the registration step performed 80 s after the start of the infusion ( $t_0$ ), followed by the prediction of the model state at 80 s and 360 s after  $t_0$ . It can be observed that the model accurately represents the flow up to  $t_0 + 80$  s, after which a discrepancy appears at the first flow front, whose velocity is higher than that measured by the camera. This trend emerges when the second valve is opened, suggesting that variations in flow rate at the injection points may not be accurately captured by the model. Indeed, during the experiment, the control parameter is the resin flow rate (up to a maximum pressure), whereas the boundary condition of the high-fidelity model is pressure, leading to an overestimation of the flow rate in the simulation. As a consequence, at the end of the injection, a slight deviation in the position of the dry zones is observed. The geometry of these zones also differs slightly, in that the model predicts visible defects both above and below the part, whereas the experiment shows dry zones only on the underside. This difference arises because the upper dry zones are filled after the resin front has passed and during the curing phase, which is not considered here. Nevertheless, the discrepancies observed between the real-time predictions and the experimental observations are considered sufficiently small (with an error on the order of 5% in both position and time) to be regarded as industrially acceptable.



**Fig. 17.** Overview of results on the infused plate with the second valve opening at 150s. The left column contains the segmentation of the resin front (with the camera image in black and white, the resin segmentation in green, the prediction in dark blue, and the intersection in blue/green), while the right column contains the model prediction seen from above and below. The first line contains the model parameters registration step, the following lines are the predictions of future states. For the latter, the corresponding segmentation is also reported.

## 2. Infusion of 6m<sup>2</sup> proof-of-concept part

The objective here is to assess the ability of the digital shadow approach to adapt to a more complex geometry and material assembly. The part under study (Figure 3) represents configurations and levels of complexity that are representative of potential industrial applications. Its approximate dimensions are 2 m × 3 m, and it includes reinforcement features in the form of stiffeners, which introduce

additional complexity. Furthermore, the curvature radius requires intrinsic and extrinsic optical calibrations in order to enable projection of the digital shadow results onto the part geometry with sufficient accuracy. As in previous cases, flow rate, heat flux, and vacuum sensors were implemented. The overall system is managed by the hardware architecture presented in Section 2.1. The parameters selected for the numerical design of experiments are the opening time of the second valve, and the permeability of the reinforcement in the direction perpendicular to the main flow, Figure 18, illustrates the real-time prediction of dry zone locations during the process as provided by the digital shadow. Experimentally, after cutting the part, dry zones were observed in the same areas, with a level of accuracy considered sufficient for industrial purposes.

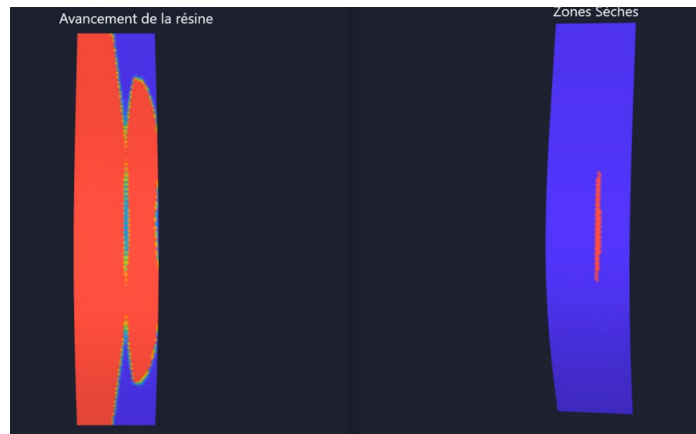


**Fig. 18.** Digital shadow result : Position of predicted resin front flow (left) and associated dry spot position (right) 5 minutes after current time.

## Conclusions and Perspectives

The infusion digital shadow, developed using a 5D methodology, enables not only the monitoring of key process parameters, but also the observation of dry spots on inaccessible surfaces. It further allows the real time prediction of the position of these areas on the final part if the infusion strategy is maintained, and the virtual testing of alternative strategies with the aim of eliminating these dry areas before they actually occur. For a unique one-product part, the dataset required to build the metamodel is based on the generation of several high-fidelity simulations (here performed using PAM-RTM© software). The accuracy of these simulations is not necessarily expected to be high, as a phase of recalibration of the metamodel is performed based on the experimental resin front. In addition, the use of camera-based sensors and other process sensors is required.

Sensitivity analyses with respect to experimental parameters, reflecting discrepancies between simulation datasets and actual infusion conditions, demonstrated that the tool is sufficiently robust to predict dry areas with an accuracy that remains industrially relevant, even under unfavorable conditions.

The main limitation of the approach lies in the number of initial parameters that must be identified. The integration of additional relevant sensors to further recalibrate the models would therefore be beneficial. Moreover, in the present study, only the ramp opening parameters were considered adjustable. In practice, the number of controllable parameters may be significantly higher, particularly when addressing larger and more complex geometries. Therefore, the choice of the most representative parameters is crucial for the success of the used approach.

## Acknowledgments

This study is a part of the MONOCLE project led by IRT Jules Verne (French Institute of Research and Technology in Advanced Manufacturing). The authors wish to thank the industrial partners of this project: Naval Group, Sicomin, Iqanto, PCMI and Bureau Veritas.

---

**References**

- [1] C. Le Gleuher, C. Buchmann, K. Schlegel, A. Friedberger : (2018). « Advanced Flow Front And Cure Monitoring Using High Frequency Technology », *SAMPE Europe Conference 2018 Southampton*
- [2] N. Gupta, “Fiber optic sensors for monitoring flow in vacuum enhanced resin infusion technology (VERITy) process,” *National Aerospace Laboratories, Elsevier, Bangalore, 2008* .
- [3] Luna Inc., “*Engineering Note EN-FY1318 Measuring Liquid Level Using Fiber Optic Sensing*,” 13 08 2013
- [4] N. Pantelelis, “Quality Monitoring and Process Control in CFRP Production”, *9th CFK-VALLEY STADE CONVENTION 2015 16-17 June 2015, Stade, Germany*
- [5] P. le Bot, G. Lebreton, N. Siddig, P. Couarraze, O. Fouché, C. Sébastien, A. De Fongalland, F. Cara, P. Gerard, “Anomaly detection during thermoplastic composite infusion: Monitoring strategy through thermal sensors,” in *Key Engineering Materials, Achievements and Trends in Material Forming*, vol. 926, 2022, pp. 1423–1436
- [6] P. Wang, J. Molimard, S. Drapier, A. Vautrin, J.C. Minni, « Monitoring the resin infusion manufacturing process under industrial environment using distributed sensors », *Journal of Composite Materials 0(0) 1–16, 2011*
- [7] P. Venegas, I. Ortiz de Mendibil, A. Montero and J. Aurrekoetxea, “Quality control by Infrared Thermography of the infusion manufacturing process of composite automotive specimens”, *13th international conference on quantitative infrared thermography 2016, july 4-8, gdańsk, Poland*
- [8] Q. Qi, F. Tao, T. Hu, N. Anwer, A. Liu, Y. Wei, L. Wang, A. Nee, “Enabling technologies and tools for digital twin”, *Journal of Manufacturing Systems, Volume 58, Part B, 2021*
- [9] P. Le Bot, D. Lecointe, N. Sidigg, O. Fouché, Le Guennec Yves, I. Abdullah, F. Niget Florent, C. Marchand Christophe, “Digital shadow dedicated to resin infusion filling process of composites parts”, *ECCM21, Nantes, July 2024*
- [10] ISO 23247-1:2021 Automation systems and integration — Digital twin framework for manufacturing
- [11] <https://docs.pytorch.org/vision/main/models/deeplabv3.html>
- [12] Y. Xie, T. Takikawa, S. Saito, O. Litany, S. Yan, N. Khan, S. Sridhar, “Neural fields in visual computing and beyond”. In *Computer graphics forum* (Vol. 41, No. 2, pp. 641-676).
- [13] M. Tancik, P. Srinivasan, B. Mildenhall, S. Fridovich-Keil, N. Raghavan, U. Singhal; “Fourier features let networks learn high frequency functions in low dimensional domains”; *Advances in neural information processing systems*, 33, 7537-7547
- [14] P. Mulye, E. Syerko, C. Binetruy, and A. Leygue, “A novel finite element based method for predicting permeability of heterogeneous and anisotropic porous microstructures”, *Materials*, MDPI.